Supporting Information

Green Composite Papers via Use of Natural Binders and Graphene for PEM Fuel Cell Electrodes

Sajjad Ghobadi [*,†,‡], *Lale Işıkel Şanlı* [†,§], *Rokhsareh Bakhtiari*[†], *Selmiye Alkan Gürsel*[†,§]

† Faculty of Engineering and Natural Sciences, Sabanci University, University Street, Tuzla, 34956 Istanbul, Turkey

‡Present Address: Department of Chemical and Life Science Engineering, Virginia Commonwealth University, 737 North 5th Street, Biotech 8, 23219 Richmond, Virginia, USA

§Sabanci University Nanotechnology Research and Application Center (SUNUM), Sabanci University, University Street, Tuzla, 34956 Istanbul, Turkey

*Email Address: ghobadi@sabanciuniv.edu & ghobadis@vcu.edu

Number of Pages: 9

Number of Figures: 4

Number of Tables: 2

1. Detailed preparation steps of graphene/cellulose/carbon fiber composite papers

As an extended description on electrode assembly the process can be further categorized in three steps. (**Figure S1**)

1) Starting from cellulose precursor, the cellulose/carbon fiber papers were prepared via wet-laying of their aqueous suspension.

2) Phase inversion of the papers was followed leading to partial elimination of cellulose fibers in the structure.

3) Then, the graphene solution in *iso*-propanol was air-sprayed over the cellulose/carbon composite paper.

The ternary graphene/cellulose/carbon fiber composite papers were then dried in 60°C oven for 1 hour. Afterwards, the commercial Pt/C 20 wt% Pt catalyst *iso*-propanol solution was air sprayed on one side of the paper for electrode preparation purpose.

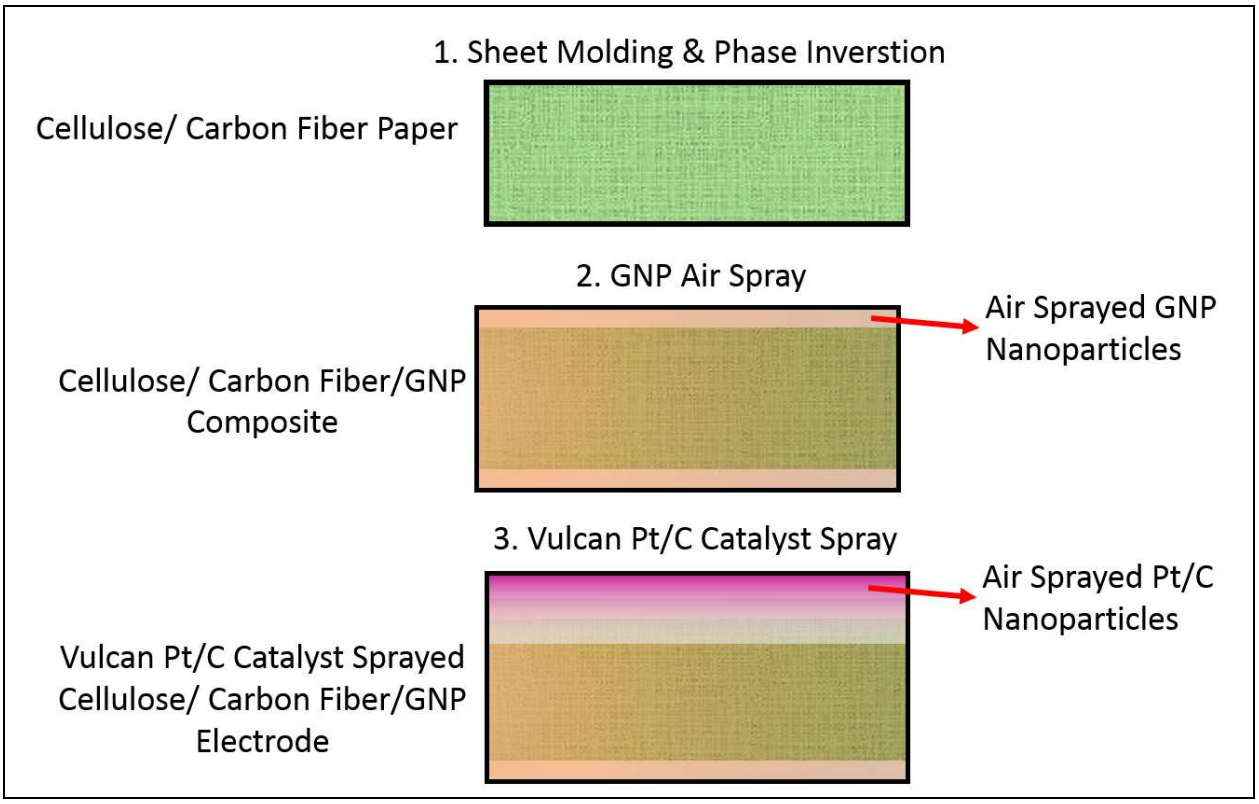

Figure S1. Step-by-step schematic view of electrode assembly process

2. Mechanical property analysis of graphene/cellulose/carbon fiber composite papers

The mechanical properties of composite papers were studied by a UTM device. The grip set was chosen for such measurement was consisted of pressurized elastomeric grips, suitable for thin films. A thin film sample compatible load cell of 200 N capacity was used for the tension measurements. For each sample 5 respective specimens of 50 x 20 mm dimensions was prepared. The samples were further trimmed at their edges in order to prevent any stress concentration zone appearance.

The Young's modulus (E) was calculated by linear curve fitting at the elastic region ($\varepsilon<0.02\%$). The slope of the fitted line represents the modulus according to the following equation: $E= (\sigma_2-\sigma_1)/(\varepsilon_2-\varepsilon_1)$

Where σ and ε are the stress and strain, respectively. The average R_2 values of the fitted curves can be found in **Table S1**. Tensile strength (τ) as the highest stress applied on the specimen before failure.

As shown in **Figure S2**, the tension test analysis of various samples revealed that via phase inversion significantly influenced the Young's modulus and strain at break of the samples in a positive manner (**Table S1**). However, although the tensile strength of phase inverted samples were higher than that of neat sample, the relative value was decreased upon increasing the ionic liquid content.

The elastic modulus (E) of phase inversion samples was higher than the neat sample due to elimination of low modulus cellulose from the material through the process. By increasing the ionic liquid, the fraction of extracted cellulose was increased resulting in higher modulus, which it reached its peak for P70 sample (@ 0.584 MPa) with highest used ionic liquid content.

Table S1 Mechanical properties of graphene/cellulose/carbon fiber composite papers

Sample	**E (MPa)**	**R2**	**τ (MPa)**	**ε @ break (%)**
C80 (Neat)	0.399 ± 0.1	0.998	0.0135 ± 0.005	0.52 ± 0.02
P20	0.304 ± 0.05	0.996	0.08 ± 0.01	2.12 ± 0.02
P50	0.353 ± 0.1	0.998	0.056 ± 0.04	1.37 ± 0.03
P70	0.584 ± 0.07	0.999	0.051 ± 0.01	4.383 ± 0.005

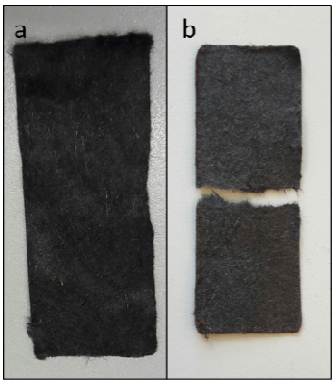

Figure S2. The UTM testing specimen a) before and b) after analysis

Tensile strength study revealed that the value was increased upon phase inversion by over 6 times fold only by using 20% IL phase inversion media in comparison with the neat sample. However, by elimination of higher fractions of cellulose using high IL content media (P50, and P70 samples) the applied tension force was mitigated by slipping of the carbon fibers due to lack of cellulose binder in the hybrid material. Thus the tensile strength was reduced at high IL-content phase inverted samples. This phenomenon was also found responsible for the samples' behavior in terms of strain at break.

Although the cellulose binder content in P70 was lower than the rest of the samples, it showed the highest ultimate strain value. Such behavior can be addressed in a way that since the carbon fibers are in direct contact without any load transfer component, it was expected to show more rigid behavior. However, the carbon fiber slippage was the responsible factor resulting in higher ultimate strain.

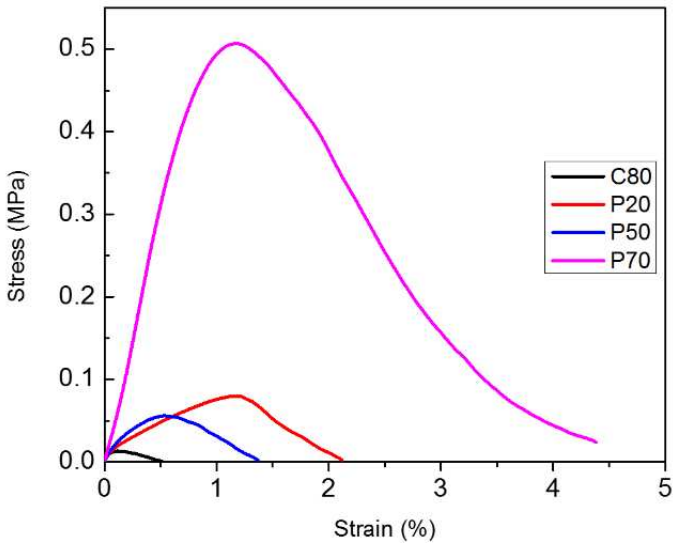

Figure S3. Stress-strain graph of sheet molded papers

3. Comparative study with respect to commercial GDLs

As shown in **Table S2**, the prepared GDL by the presented approach showed superior power generation in comparison with most of the commercial GDLs by at least over 100%. Nevertheless, the cellulose/carbon fiber MEA systems, kept their consistent improved performance even at relative humidity (RH%) values of lower than 100%.

Although the study with higher maximum power density, with ZBT commercial GDL, used the same conditions to this study's tests, only less than 15% performance improvement was reported compared to this study's GDLs.

In the case of commercial GDLs water management, specially PTFE coating and high RH values, was crucial for a reliable performance due to their flooding or dehydration problems. Whereas, the cellulose/carbon fiber GDLs, despite the 50% reduction in RH kept their high performance by over 85%.

Table S2 Comparative analysis of the fuel cell performance of the current study's GDLs with commercial counterparts

Reference	GDL	Operating Temperature (°C)	Relative Humidity (%)	Fuel	Pt loading (mg/cm^2)	Max Power Density (mW/cm^2)
[1]	Carbon Cloth	65	100	H_2/Air	0.4	220
[2]*	ZBT	80	90	H_2/O_2	0.36	1080
[3]*	PE-704 SGL®	60	60	H_2/Air	0.4	460
This Study	Cellulose /Carbon Fiber	60	50	H_2/O_2	0.5	855
This Study	Cellulose /Carbon Fiber	60	75	H_2/O_2	0.5	784
This Study	Cellulose /Carbon Fiber	60	100	H_2/O_2	0.5	726

* PTFE coating applied

4. Durability and extended current scan analysis

The durability analysis of the prepared composite GDLs were done up to 50 hours (**Figure S4-a to d**). It was shown that the open circuit value was returned to its initial state with full recovery. Therefore, reliable performance of the MEA was achieved through multiple cycles.

While the peak current density reached to over 2200 mW/cm^2 during the initial cycles, it was diminished approximately by 50% after 50 hours of operation. Consequently, the peak power density recorded at 20^{th} hour cycle gradually declined from 541 to 266 mW/cm^2 as the operation time reached the 50 hours. This phenomenon could be attributed to the Pt catalyst leaching and deactivation during the durability test period. Nevertheless, as it was also reported in power

density measurement at 0.6V during recurring cycles (Figure S4-f), that the MEA performed consistently based on the recorded data at the desired voltage.

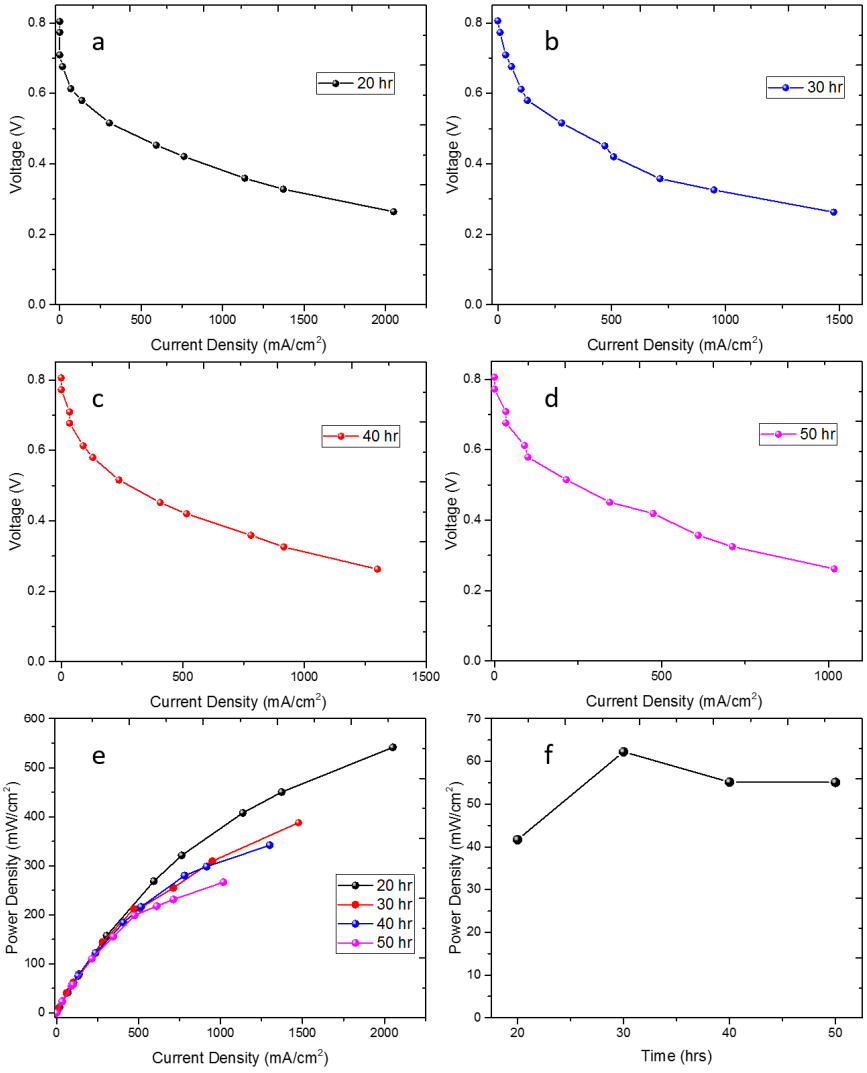

Figure S4. Polarization curves of P80 GDLs for durability @ 100%RH at a) 20 hrs, b) 30 hrs, c) 40 hrs, d) 50 hrs, e) Power density screening of durability test, and f) Power density screening at 0.6 V voltage.

References

1. Lai, Y.-C., et al., *Sputtered Pt loadings of membrane electrode assemblies in proton exchange membrane fuel cells.* International Journal of Energy Research, 2012. **36**(8): p. 918-927. DOI:10.1002/er.1883
2. Marinkas, A., et al., *Enhanced stability of multilayer graphene-supported catalysts for polymer electrolyte membrane fuel cell cathodes.* Journal of Power Sources, 2015. **295**: p. 79-91. DOI: 10.1016/j.jpowsour.2015.06.126
3. Han, M., S.H. Chan, and S.P. Jiang, *Investigation of self-humidifying anode in polymer electrolyte fuel cells.* International Journal of Hydrogen Energy, 2007. **32**(3): p. 385-391. DOI: 10.1016/j.ijhydene.2006.08.034